Characteristics of Wind Pressures on Large Cantilevered Roofs: Effect of Roof Inclination

J. G. Zhao and K. M. Lam*

Department of Civil Engineering, The University of Hong Kong, Hong Kong, China

Manuscript for: Journal of Wind Engineering and Industrial Aerodynamics
A Special Issue for APCWE V
Number of pages: 13
Number of tables: 0
Number of figures: 7

---

*Corresponding author: Dr. K. M. Lam,
Department of Civil Engineering,
The University of Hong Kong, Pokfulam Road, Hong Kong
Fax: (852) 2559 5337
e-mail: kmlam@hku.hk

Characteristics of Wind Pressures on Large Cantilevered Roofs: Effect of Roof Inclination

J. G. Zhao and K. M. Lam*

Abstract

Wind pressure distributions on both surfaces of a cantilevered roof are measured on a wind tunnel model. The investigation covers a down-sloping roof configuration at -5^o roof angle and two up-sloping roof configurations of roof angles 5^o and 10^o. The results supplement an earlier study made on a horizontal roof. The wind pressure pattern on the upper surface of an up-sloping roof suggests that there exists a preferred mode of flow separation on that surface. The pattern shows two localized regions of high suction which are separately located towards the two ends of the roof span. On the up-sloping roofs, this pressure pattern is observed in the time-averaged mean distribution as well as during the occurrence instant of a peak total uplifting force on the roof. On the horizontal roof, this particular pattern of flow separation is not obviously observed in the time-averaged mean wind pressure pattern but is revealed by the conditional sampling technique which captures the wind pressure distribution during the generation of a peak uplifting force on the roof. The wind pressure signals are analyzed to study the characteristics of the total wind force on the roof and also the wind forces on individual roof surfaces.

Keywords: Cantilevered roof, Wind pressure, Grandstand roof

1. Introduction

Characteristics of wind pressures on a large horizontal cantilevered roof were investigated recently by the present authors [1, 2]. Simultaneous pressure measurements were made on both surfaces of a wind tunnel roof model. Mean and peak roof pressure and roof forces were analysed with conventional statistical methods and the conditional sampling technique. The results suggest that the uplifting force is contributed by wind pressures on both roof surfaces with a larger contribution from the upper surface. This is particularly the case for the generation of peak roof lift.

Apart from commonly used as grandstand roofs, large cantilevered roofs are increasingly used in metropolitan cities as huge canopies overhanging from large building developments with a purpose to provide sun shading or to act as a noise barrier to highway noise. The large uplifting pressure and forces found on these roofs are usually due to the separation of wind flow at the leading edge. Wind pressures on both roof surfaces contribute to the total roof lift and this leads to complications in cases where wind tunnel loading information is obtained separately for individual roof surfaces. A discussion on this issue in relation to wind effects on the perimeter eaves of low-rise buildings was made in Stathopoulos [3].

This paper extends the investigation to large cantilevered roofs at non-horizontal inclination angles. As in the previous study [2], simultaneous pressure measurements are made on the upper and lower roof surfaces with an electronic pressure scanning system. The effect of the roof inclination angle on the pressure pattern and wind forces on these roofs is investigated.

2. Wind tunnel experiment

The present investigation made use of a wind tunnel model of a cantilevered roof [2]. Details of the wind tunnel test and the experimental instrumentation have been described in Lam and Zhao [2]. Model of the roof and the stepped grandstand is shown in Fig. 1. The roof

model was rectangular in shape, 780 mm wide and 150 mm deep. It was cantilevered at its rear edge at a height of 180 mm above the wind tunnel floor. The geometric length scale was targeted at 1:100. The stepped grandstand model had a maximum height of 135 mm. The blockage ratio was 0.75.

Experiments were carried out in the boundary layer wind tunnel of the Department of Civil Engineering, The University of Hong Kong. The test section of the wind tunnel was 3 m wide and 1.8 m high. Triangular spires and 8 m fetch of roughness elements were used to simulate natural wind conditions at a target scale of 1:100. Characteristics of the simulated wind have been documented previously [1, 2]. The lower part of the mean wind speed profile followed closely the log-law with an aerodynamic roughness length of z_o = 1.1 mm, or 0.011 m in full scale. The upper part of the mean wind speed profile could be described by a power law with an exponent of 0.19. The turbulence spectrum measured at a height roughly equal to the roof height collapsed well with the ESDU spectrum [4]. The value of the integral scale of turbulence which produced the best fit is 0.27 m in model scale, or 27 m in full scale. The turbulence intensity at the roof height was 0.12.

There were 78 pairs of pressure taps installed on both upper and lower roof surfaces on a grid of 13 points × 6 points [2]. At each grid point, the pressure taps on the two roof surfaces were installed at the same location. Near-simultaneous pressure measurements were made on the total 156 pressure taps with five 32-port electronic pressure scanners (PSI Inc.). The sampling rate was 100 Hz per tap and the sampling period was 60 seconds. At a length scale of 1:100 and a target velocity scale of 1:4, the full scale sampling rate and period were 4 Hz and 25 minutes. A discussion on the accuracy of the pressure measurement has been made in Ref. [2].

Experiments had been carried out on the wind tunnel model with the roof mounted at the horizontal position. Those results have been reported in Ref. [2]. In the present investigation, experiments were carried out at three other roof inclination angles θ. These included a down-sloping roof at $\theta = -5^o$, and two up-sloping roof configurations at $\theta = 5^o$ and 10^o.

3. Results and discussion

Fig. 2 shows the distribution of time-averaged mean wind pressure on the upper and lower roof surfaces for the three sloping roofs under normal wind incidence from the front (wind angle, α = 0^o). The previous results obtained on the horizontal roof are also shown [2]. The pressure contours are presented in terms of pressure coefficients with the velocity pressure at the roof height as the reference dynamic pressure. The figure also shows the net mean pressure coefficient on the roof due to the combined effect of the upper and lower roof surfaces:

$$\overline{C}_{p,net} = \overline{C}_{p,upper} - \overline{C}_{p,lower} \tag{1}$$

Since the pressure coefficients on the two roof surfaces follow the usual convection of acting from the flow onto the roof surfaces, the net pressure coefficients are defined positive in the vertically downward direction.

For the down-sloping roof, the mean wind pressure distributions on both roof surfaces are very similar to those of the horizontal roof. The entire upper roof surface is under suction. In the time-averaged sense, a rather uniformly high suction region is found along the entire span of the windward edge. The lowest pressure coefficient contour line covering that region has the value of $\overline{C}_{p,upper}$ = –1.0. The size of the bounded region is slightly smaller than that on the horizontal roof. This should be connected with the down-sloping roof angle which affects the separation of flow at the windward edge. In addition to the mean suction area, there are small regions of localized high suction at the two windward corners.

On the lower roof surfaces, upward acting pressure are mostly found. The magnitudes of the upward pressure are the largest on the windward edge and decrease on going downwind along the roof depth. The highest pressure coefficient contour at the windward edge has a level of $\overline{C}_{p,lower}$ = 0.8. This is slightly higher than that on the horizontal roof. The different behaviours of wind pressure on the upper and lower roof surfaces are due to the grandstand which channels wind flow underneath the roof and

suppresses separation. The pattern of net mean wind pressure on the down-sloping roof is very similar to that on the horizontal roof. The pressure levels are also very similar.

When the roof is inclined upward at the front, the pressure distributions on the upper surface show a different pattern. At the roof inclination of $\theta = 5^{o}$, the uniform high suction region on the windward edge found previously for the horizontal and down-sloping roofs obviously breaks up into localized regions. Two high suction regions are found centred at about 1/6 roof span from the two sides of the roof. In Fig. 2c, they are bounded by the pressure coefficient contour $\overline{C}_{p,upper} = -1.0$. At the middle span of the roof, the suction levels are lower and a narrow strip of the windward edge is under suction of $\overline{C}_{p,upper} < -0.8$. At the larger inclination angle of $\theta = 10^{o}$ (Fig. 2d), the two regions of high suction are clearly observed, each with a local valley of negative pressure bounded by closed contours of $\overline{C}_{p,upper} = -1.0$ and -0.8. At the middle part of the roof span, no region of high suction characteristic of flow separation can be found.

On the lower surfaces of these up-sloping roofs, the pressure distributions exhibit a pattern similar to that of the horizontal roof or the down-sloping roof. This suggests that the grandstand exerts a more dominant effect on the flow underneath the roof than the roof inclination angle. The small blockage of the lower roof surface to the wind flow, however, leads to slightly larger upward wind pressure on the front edge of the roof.

Distribution of the net mean roof pressure follows a pattern similar to the distribution pattern of the upper roof pressure. For the two up-sloping roofs, the two localized regions of high net upward pressure are observed in Figs. 2c and 2d. The net pressure coefficients in the two valleys of contour lines reach a minimum value around $\overline{C}_{p,net} = -1.6$. On the down-sloping roof and the horizontal roof, these two localized valleys are not observed. Instead, a single region of highest net upward pressure is found at the middle half roof span along the windward edge. A minimum value around $\overline{C}_{p,net} = -1.8$ is found there for the net roof pressure coefficients (Figs. 3a,b).

In the previous study on the horizontal roof [2], the conditional sampling technique has been used to investigate the wind pressure pattern on the roof surfaces when a peak

uplifting force is occurring on the roof. The time history of the total roof force was obtained from an integration of the near-simultaneous pressure signals at all tap locations over both surfaces of the roof. Following the sign convention of wind pressure in Eq. (1), the roof force was defined positive in the vertically downward direction. The instants of peak uplift were taken as the valleys in the time signal of the roof force with a level lower than the mean force value by more than three times the standard deviation:

$$F(t) = \sum_{upper}^{surface} p_i(t) A_i - \sum_{lower}^{surface} p_i(t) A_i$$
$$F(t_{peak}) < \overline{F} - 3\sigma_F \tag{2}$$

The pressure distributions on the roof surfaces at those 10 to 15 instants were then averaged to represent the typical pattern of wind pressure when a peak uplift is occurring.

It was found that on the upper surface of the horizontal roof, the sampled pressure pattern is obviously different from the mean pressure pattern. The former pattern, which is repeated here in Fig. 3b, shows two separated localized regions of highest suction ($C_{p,upper}$ < –1.2) towards the two ends of the roof span. The location and shapes of these two regions are similar to those found on the mean pressure pattern on the up-sloping roofs (Figs. 2c,d).

In this study, the same conditional sampling technique is applied to obtain the pressure distributions on the surfaces of the sloping roofs at the occurrence instants of peak roof uplift. The results on the upper roof surface are shown in Fig. 3. The results for the lower roof surfaces show that the distribution of the conditionally sampled wind pressure has a pattern very similar to that of the mean wind pressure pattern except that the pressure levels are higher. This has been observed for the horizontal roof [2] and those results are not presented here. Discussion is mainly made on the pressure on the upper roof surface.

For the up-sloping roofs, on the upper roof surface, the two localized regions of high suction found in the mean pressure distribution pattern are observed with a much higher levels of negative pressure (Figs. 3c,d). The inner-most pressure coefficient contour lines in the valleys have a level of $C_{p,upper}$ < –1.2 and even –1.4 on the more inclined roof at θ = 10°. On the down-sloping roof, the two localized high suction regions are not

observed. Instead, there are localized regions of high suctions scattered along the windward span of the roof.

The explanation for this observation is related to the mode of flow separation along the windward edge of the roof. In the instantaneous sense, wind does not separate uniformly along the entire roof span. Separation occurs only over a part of the roof span. On the horizontal roof and especially true for the down-sloping roof, these smaller-scaled separations occur mostly on the windward span of the roof without any preferred locations. When the pressure distribution is time-averaged, a uniform region of high negative pressure results at the windward edge almost along the entire roof span (Figs. 2a,b). On the up-sloping roofs and also for the horizontal roof, it appears that the mode of separation which leads to the highest suction on the roof surface is connected with a highly localized separation occurring towards either ends of the roof span. This preferred localized high suction region is centered at about 1/6 roof span distance from one side of the roof and covers an area of about 1/6 roof span by 1/3 roof depth.

Figs. 4a and 4b shows the conditionally sampled pressure distribution on the upper roof surfaces of the down-sloping roof and up-sloping roof at 5^o when wind incidence is from the rear of grandstand ($\alpha = 180^o$). The two localized regions of high suction are now observed on the down-sloping roof. This is because at this opposite direction of wind incidence, the down-sloping roof is inclined upwards to the incoming wind. The particular mode of separation is thus connected with the angle of attack with respect to the incoming wind. The pressure pattern on the up-sloping roof is now similar to that found on the down-sloping roof at normal wind incidence from the front ($\alpha = 0^o$).

Fig. 5 shows the distribution of mean wind pressure on the upper roof surfaces and the net mean wind pressure at an oblique wind incidence angle of $\alpha = 30^o$. The patterns on the down-sloping roof are similar to those found on the horizontal roof [2]. The pressure contour lines on the upper roof surface do not show any obvious hills or valleys. For the up-sloping roofs, however, the pressure contour lines on the upper roof surfaces show a valley of high suction running from the windward roof corner along a direction at about 30^o from the windward roof span. This suggests the presence of some kinds of conical

vortices originating from the windward roof corner. The negative pressures found in the valley of suction reach very high levels. The levels are even higher on the more inclined roof at $\theta = 10^{o}$. At the same time, the upward pressures on the lower roof surface are higher on the up-sloping roof. As a result, the highest negative net wind pressures found on the up-sloping roofs are much higher than those found on the down-sloping and the horizontal roof. In Fig. 5, the minimum net wind pressure coefficient found on the down-sloping roof is at $\overline{C}_{p,net} = -1.6$ and is found on a narrow strip along the upwind half of the front roof edge. On the up-sloping roofs, the most negative wind pressure coefficient is found at the upwind roof corner and the value is below $\overline{C}_{p,net} = -2.4$.

As discussed earlier by way of Eq. (2), the time signal of the total roof force is obtained from the pressure signals. The mean and peak values of the roof forces are computed and the variations with wind direction are shown in Fig. 6. The standard deviations of the force fluctuations are also shown in the figure. At most wind directions, the roof is under an uplifting force, that is, a force with a negative value. However, the up-sloping roofs are under a small net downward force around $\alpha = 120^{o}$. This is mainly due to a large downward force on the lower roof surface. It appears that at this wind direction near parallel to the roof span, the effect of the grandstand is weak and the upwind angle of attack of the lower roof surface leads to some flow separation from the surface. As for the uplift, the largest upward roof force is always found at normal incidence from the front. The magnitude of this uplift increases as the roof inclination angle increases from down-sloping to up-sloping. The values of mean net force coefficient are $\overline{C}_{F,net} = -0.95$ for $\theta = -5^{o}$; -1.24 for $\theta = 5^{o}$; and -1.30 for $\theta = 10^{o}$. On the horizontal roof, the value is $\overline{C}_{F,net} = -1.0$ [2]. The area of a single roof surface is used to derive the force coefficient.

Besides the total roof force, time histories of the forces on the upper roof surface and on the lower roof surface are obtained from an integration of the pressure signals over one surface of the roof. In Eq. (2), the upper roof surface force is defined positive in the downward direction and the lower surface force is positive when acting upwards. The relationship of the total net roof lift with the two roof surface forces is explored by

computing the cross correlation function. Fig. 7 shows the cross correlation between the total net roof force with either the upper or lower surface force for the down-sloping roof and the up-sloping roof at 5^o roof angle under some wind incidence directions. Small differences are observed between the results of the up-sloping roof and the down-sloping roof. The results for the horizontal roof [2] and for the up-sloping roof at 10^o are also very similar to the results in Fig. 7. In other words, the same time-averaged relationship applies for all roof inclination cases between the total roof lift and the forces on the two contributing roof surfaces.

At wind incidence from 0^o to 60^o, higher levels of correlation coefficients are found between the total net roof force and the upper roof surface force as compared to that with the lower roof surface force. The upper surface always plays a larger contribution to the total roof load. It appears in Fig. 7 that the contribution is even higher for the up-sloping roof. At $\alpha = 90^o$ when wind is blowing parallel to the roof span, the flow is similar to a parallel flow along a flat plate. There are very low levels of wind pressure on either roof surfaces and both roof surface forces are weakly connected to the net roof force [2].

4. Conclusion

Up-sloping and down-sloping cantilevered grandstand roofs are tested in the wind tunnel to investigate the characteristics of wind pressure and wind forces on the roof surfaces. The results supplement previous studies made on a horizontal roof by the authors [1, 2]. It is found that the wind pressure patterns on the down-sloping roof are very similar to those of the horizontal roof. On the up-sloping roofs, however, very different patterns are observed, mainly on the upper roof surface. The mean wind pressure pattern and the conditionally sampled wind pressure pattern at the occurrence instant of a peak total uplifting force on the roof suggest that there exists a preferred mode of wind separation on the upper roof surface when it is inclined at an upward angle of attack to the wind flow. Two localized regions of high negative pressure are found towards the two ends of the roof

span. For all roof inclinations, the total roof lift is found to be contributed more by the force on the upper roof surface and the relationship between them is more intimate than that with the lower roof force. Similar pressure patterns are found on the lower surfaces of all roofs. This is due to the flow channeling effect by the stepped grandstand.

Acknowledgement

The investigation is supported by a research grant awarded by the Research Grants Council of Hong Kong.

References

[1] J.G. Zhao, K.M. Lam, Occurrence of peak lift on a large cantilevered roof, Proc, 1st Int. Sym. on Wind and Structures, Cheju, Jan. 2000, 217-226.

[2] K.M. Lam, J.G. Zhao, Occurrence of peak lifting actions on a large horizontal cantilevered roof, J. Wind Eng. Ind. Aerodyn. (to appear).

[3] T. Stathopoulos, Wind loads on eaves of low buildings, J. Struct. Div., ASCE, 107 (1981), 1921-1934.

[4] Engineering Sciences Data Unit, Characteristics of atmospheric turbulence near the ground: Part 2 – single point data for strong winds (neutral atmosphere). Data Item 74031. London, ESDU, 1974.

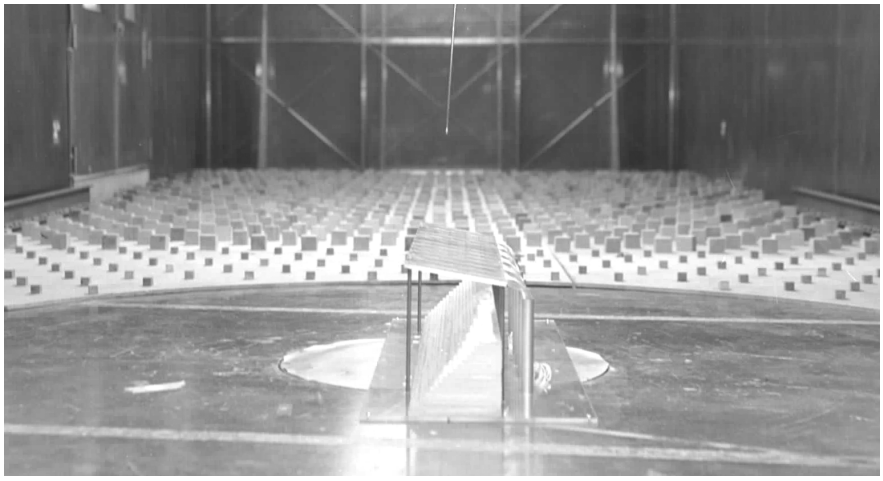

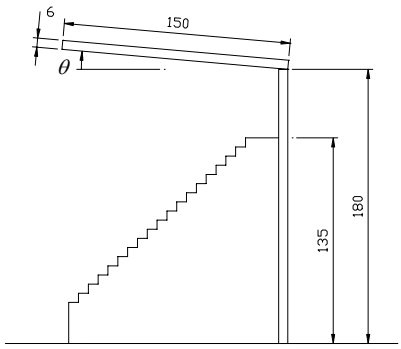

Fig. 1. Wind tunnel model of cantilevered roof and grandstand.

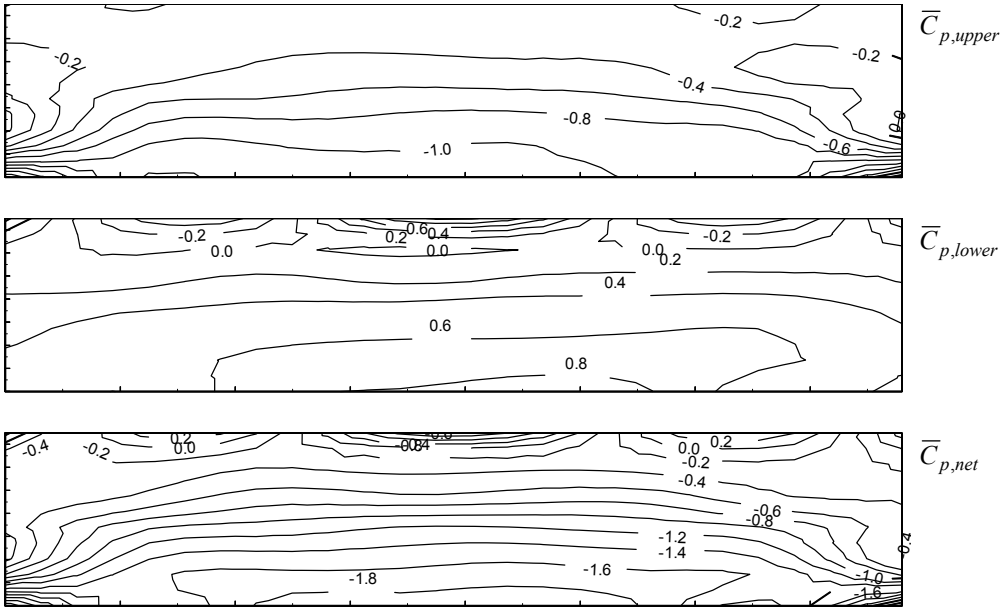

(a) $\theta = -5^{o}$ (down-sloping roof)

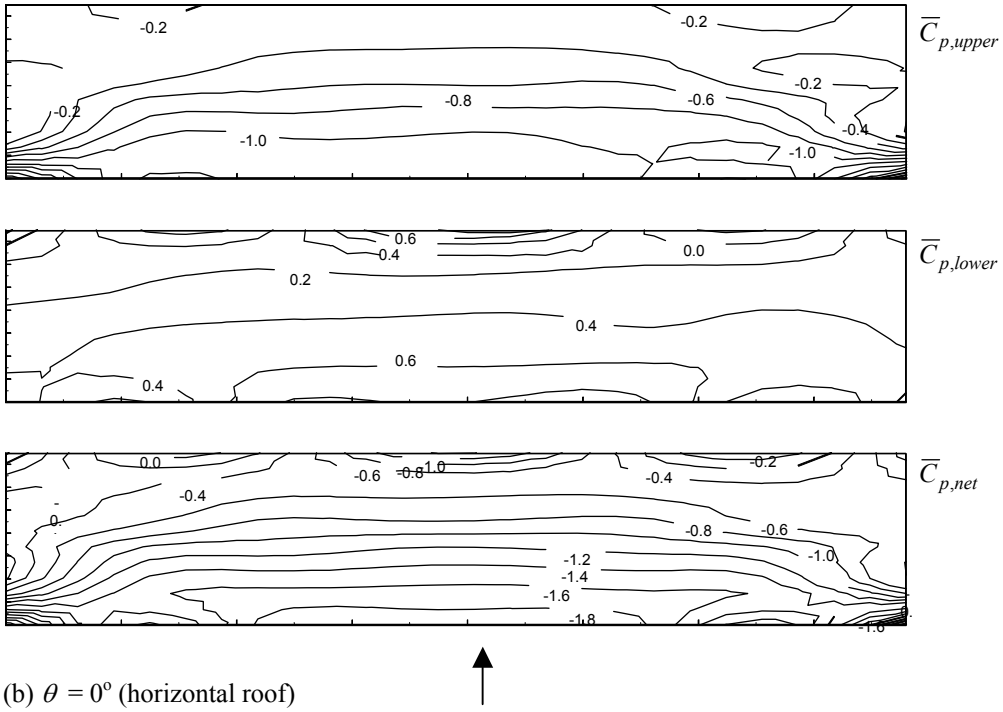

(b) $\theta = 0^{o}$ (horizontal roof)

Fig. 2. Contours of mean pressure coefficients on upper roof surface, lower roof surface, and net roof pressure. Normal wind incidence at $\alpha = 0^{o}$. Roof inclination angle: (a) -5^{o}; (b) 0^{o}; (c) 5^{o}; (d) 10^{o}.

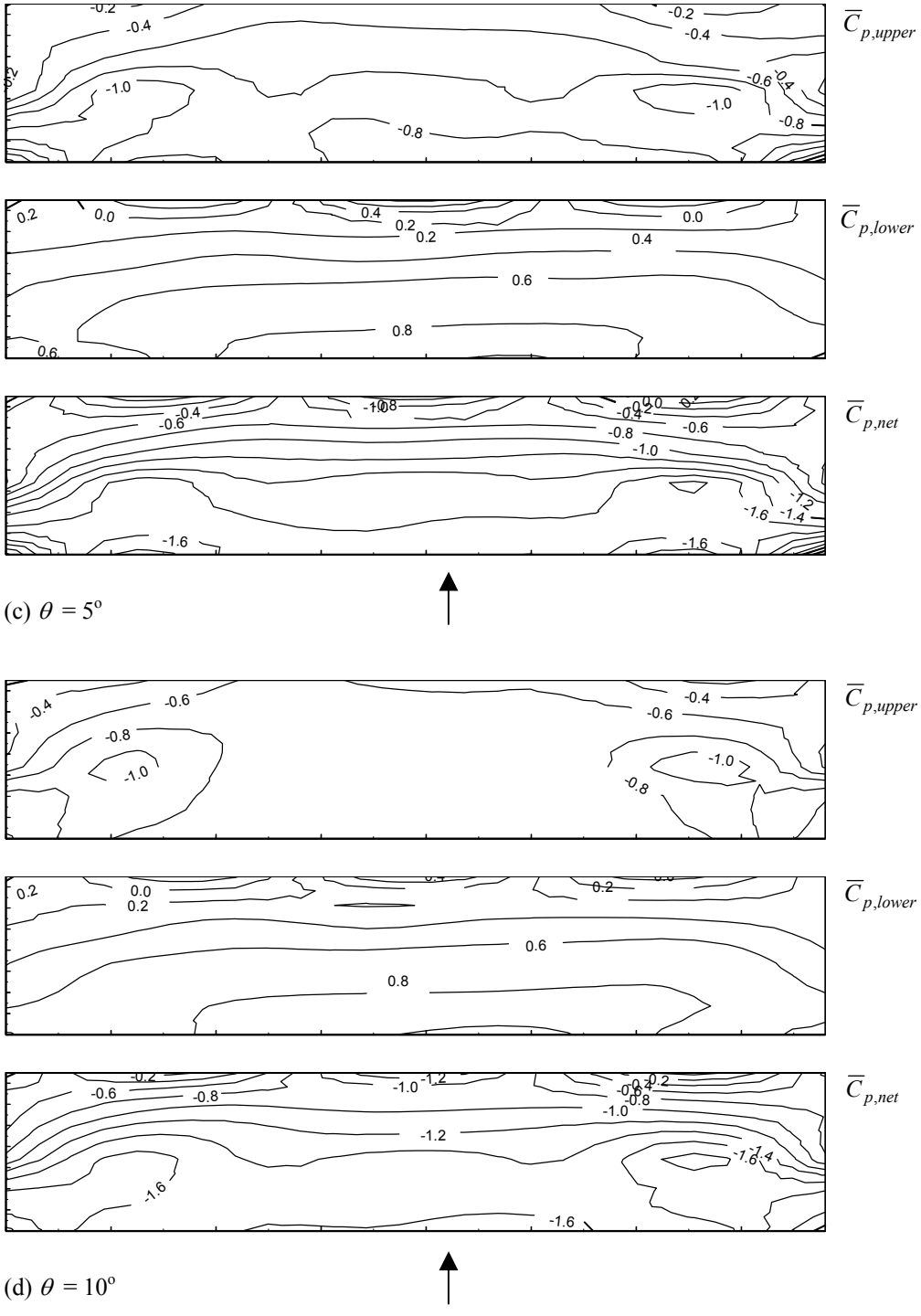

Fig. 2. Contours of mean pressure coefficients on upper roof surface, lower roof surface, and net roof pressure. Normal wind incidence at $\alpha = 0^o$. Roof inclination angle: (a) -5^o; (b) 0^o; (c) 5^o; (d) 10^o.

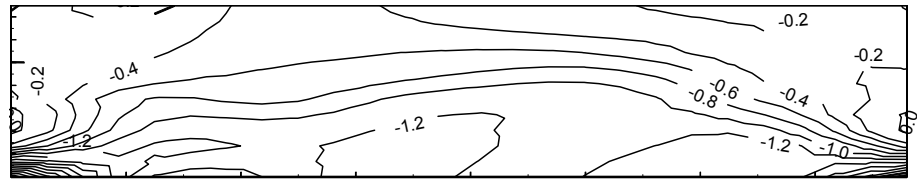

(a) $\theta = -5^{o}$ (down-sloping roof) $C_{p,upper}$

(b) $\theta = 0^{o}$ (horizontal roof)

(c) $\theta = 5^{o}$

(d) $\theta = 10^{o}$

Fig. 3. Contour maps of upper roof pressure coefficients conditionally sampled at instant of peak total roof uplift. Wind incidence at $\alpha = 0^{o}$.
Roof inclination angle: (a) -5^{o}; (b) 0^{o}; (c) 5^{o}; (d) 10^{o}.

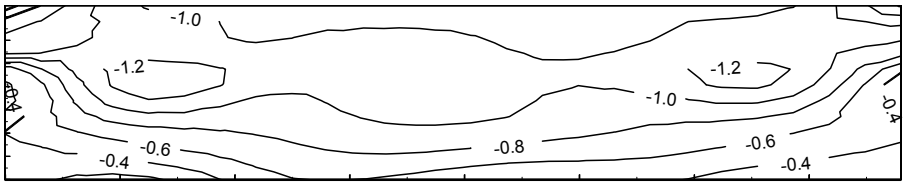

(a) $\theta = -5^{o}$ (down-sloping roof)

$C_{p,upper}$

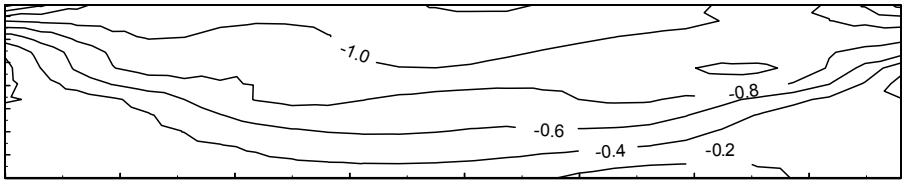

(b) $\theta = 5^{o}$ (up-sloping roof)

Fig. 4. Contour maps of upper roof pressure coefficients conditionally sampled at instant of peak total roof uplift. Wind incidence at $\alpha = 180^{o}$. Roof inclination angle: (a) -5^{o}; (b) 5^{o}.

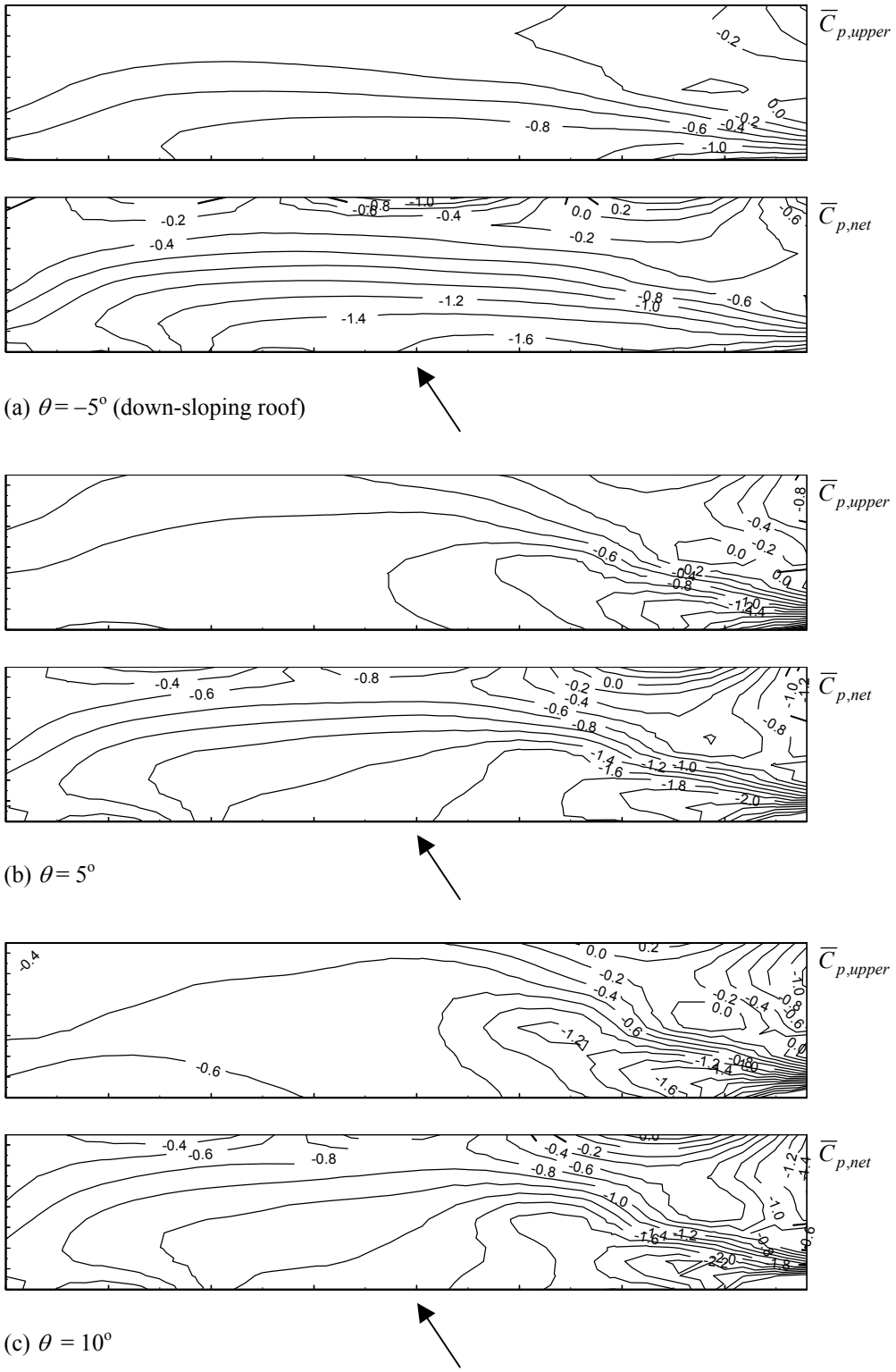

Fig. 5. Contours of mean pressure coefficients on upper roof surface and net roof pressure. Wind incidence at $\alpha = 30^o$. Roof inclination angle: (a) -5^o; (b) 5^o; (c) 10^o.

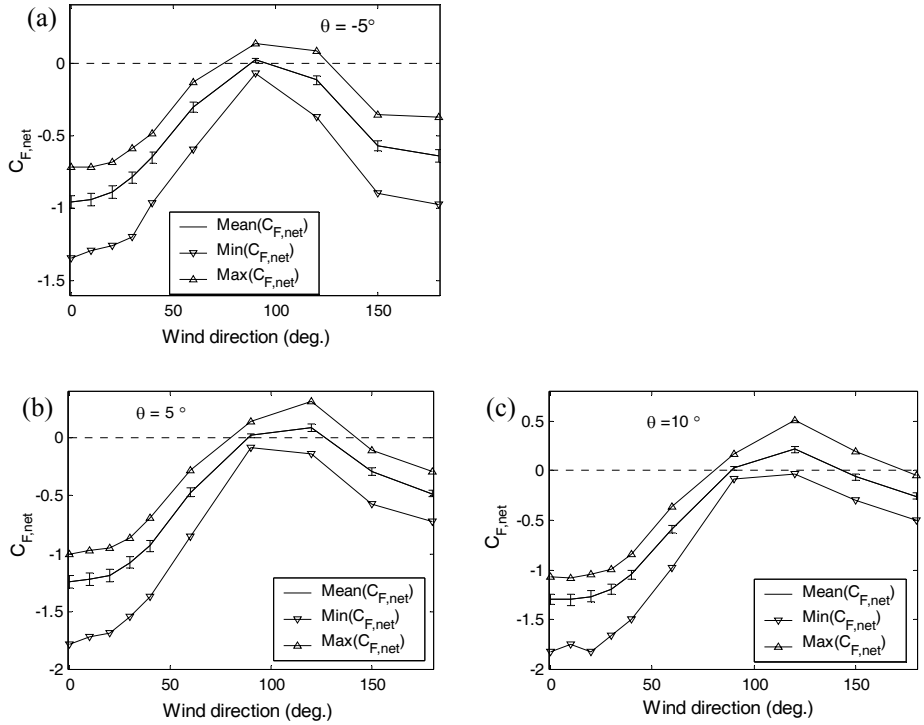

Fig. 6. Variation of mean and peak total roof force coefficients with wind angles. Middle curve is mean force coefficient with bar showing plus and minus one standard deviation. Upper and lower curves are maximum and minimum force coefficients. Roof inclination angle: (a) -5^o; (b) 5^o; (c) 10^o.

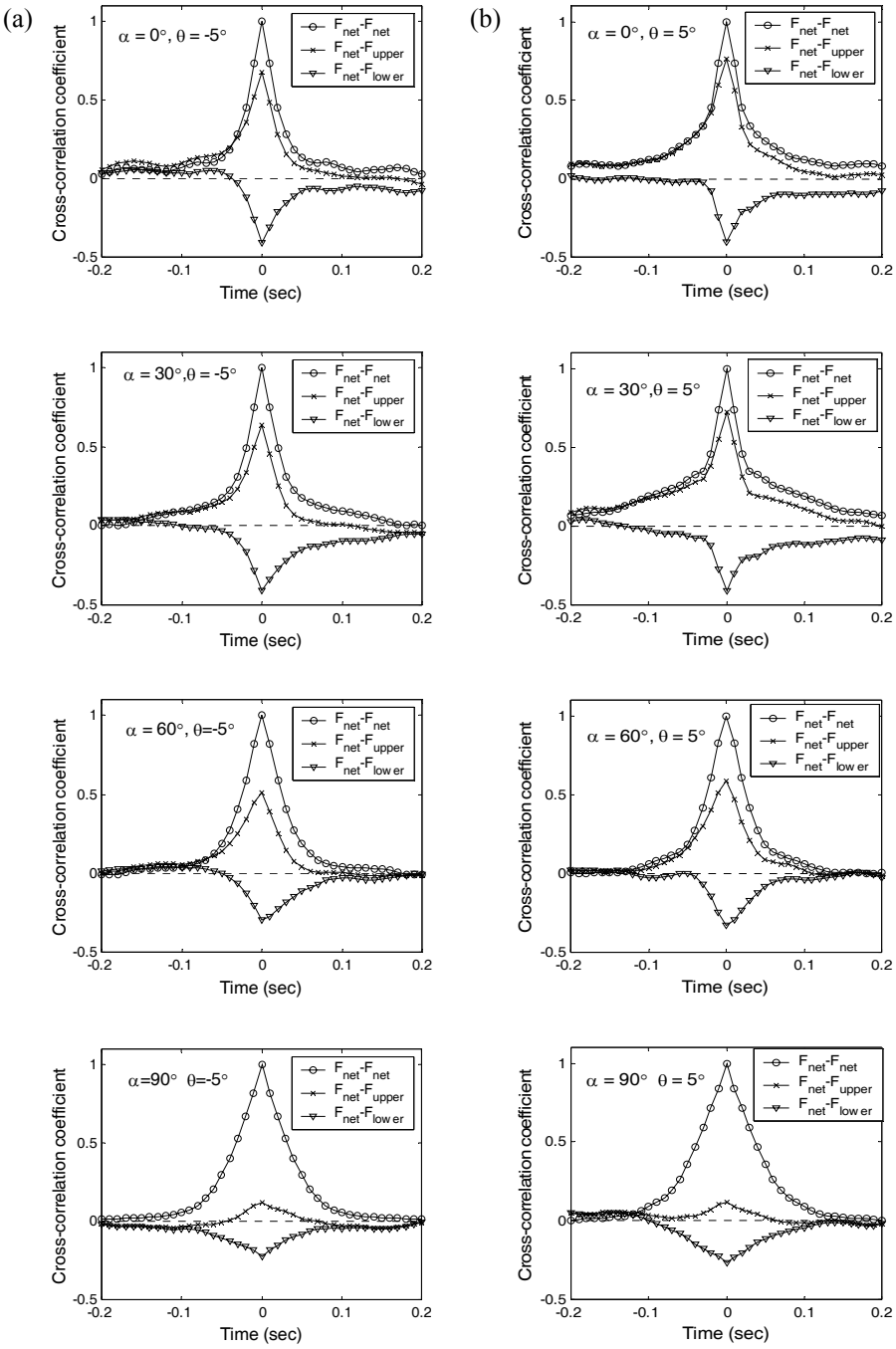

Fig. 7. Cross-correlation coefficients between total net roof force and upper/lower surface forces. Curves: o, auto-correlation of net roof force; ×, net roof force with upper surface force; ∇, net roof force with lower surface force. Roof inclination angle: (a) -5^{o}; (b) 5^{o}.